Melting of Quasi-Two-Dimensional Charge Stripes in $La_{5/3}Sr_{1/3}NiO_4$

S.-H. Lee[1] and S-W. Cheong[2]
[1]*University of Maryland, College Park, Maryland 20742 and National Institute of Standards and Technology, Gaithersburg, Maryland 20899*
[2]*Bell Laboratories, Lucent Technologies, Murray Hill, New Jersey 07974*
(Received 27 January 1997)

Commensurability effects for nickelates have been studied, for the first time, by neutron scattering on $La_{5/3}Sr_{1/3}NiO_4$. Upon cooling, this system undergoes three successive phase transitions associated with quasi-two-dimensional (2D) commensurate charge and spin stripe ordering in the NiO_2 planes. The two lower temperature phases are stripe lattice states with quasi-long-range in-plane charge correlation. When the lattice of 2D charge stripes melts, it goes through an intermediate glass state before becoming a disordered liquid state. This glass state shows short-range charge order without spin order, and may be called a "stripe glass" which resembles the hexatic/nematic state in 2D melting. [S0031-9007(97)04172-0]

PACS numbers: 71.45.Lr, 64.70.Kb, 71.38.+i, 74.72.Dn

Charge and spin ordering in real space have attracted much attention due to their role in cuprate superconductivity [1,2]. Recent neutron scattering experiments have shown that the real-space segregation of holes and spins in a stripe form is associated with the anomalous suppression of superconductivity in the La_2CuO_4 family compounds with $\sim\frac{1}{8}$ doping [3]. These findings lead to the speculation that the inelastic peaks explored earlier in superconducting cuprates [4] are due to dynamic fluctuation of these stripes. Such charge and spin stripes were first observed in the isostructural system $La_{2-x}Sr_xNiO_{4+\delta}$ by electron diffraction [5] and by neutron scattering measurements [6]. Mechanisms such as a Fermi-surface nesting [1], frustrated phase separation [2], and polaron ordering [5] have been suggested as being responsible for the formation of stripes. One of the issues is whether such an order is charge and/or spin driven. Experimental results reported so far are conflicting. The simultaneous incommensurate peaks due to charge and spin orders were found in $La_2NiO_{4.125}$ [6]. On the other hand, in $La_{1.775}Sr_{0.225}NiO_4$ the incommensurate charge peaks occur at significantly higher temperature than the spin peak, even though the in-plane charge order shows a shorter correlation length than the spin order in the compound [7].

Commensurability has significant effects for charge and spin ordering because of commensurate lock-in effect [8]. For example, suppression of superconductivity in $La_{2-x}Ba_xCuO_4$ is found when static charge and spin ordering occurs for $x = \frac{1}{8}$ [3]. $La_{2-x}Sr_xNiO_4$ compounds exhibit distinct anomalies at $x = \frac{1}{3}$ and $\frac{1}{2}$ [5,9,10]. So far, structural correlations for $La_{2-x}Sr_xNiO_4$ with $x = \frac{1}{3}$ and $\frac{1}{2}$ have been investigated only by electron diffraction on polycrystalline specimens. Such data are difficult to analyze quantitatively and lack information on magnetic correlations. In this Letter, we report the first neutron scattering measurements on a single crystal of $La_{2-x}Sr_xNiO_4$ with $x = \frac{1}{3}$, which have enabled us to extract detailed information about the order parameter and correlation lengths for this important composition. Our results "consistently" show charge order as the driving force behind the phase transitions in this compound.

We have, furthermore, discovered the intriguing 2D-melting-like transitions in this commensurate $\frac{1}{3}$ composition. The lattice of the 3D Fe^{2+}/Fe^{3+} ordering in Fe_3O_4 melts at $T \approx 125$ K in a first-order fashion, accompanied by a hysteretic discontinuity in the resistivity [11]. Recently, it has been found that there exists a strongly first order melting transition of the charge-ordered state of the 3D perovskite $Pr_{1/2}Sr_{1/2}MnO_3$ [12]. In contrast with the first-order nature of 3D melting, transitions in 2D melting can be continuous. An interesting aspect of 2D melting is the presence of a glass state (the so-called hexatic/nematic state) between the crystalline solid and liquid phases [13]. We discovered that the melting of quasi-2D charge stripes in $La_{5/3}Sr_{1/3}NiO_4$ resembles the solid-hexatic/nematic-liquid transition in 2D melting.

A large boule of single crystalline $La_{5/3}Sr_{1/3}NiO_4$ ($\sim$7 mm in diameter and $\sim$80 mm long) was grown using the floating zone method. The seed crystal and the polycrystalline feed rod were rotated at $\sim$30 rpm in opposite directions, and both with molten zone were moved downward at the speed of $\sim$5 mm/h. The top of the boule (8 mm long with a weight of 3.5 g) was cut for neutron scattering measurements. The sample mosaic spread was 0.7°. The neutron scattering experiments were performed on a thermal neutron triple axis spectrometer BT2 and a cold neutron triple axis spectrometer SPINS at the NIST reactor. Fixed incident and final neutron energies were selected to be 14.8 meV for measurements on BT2 and 5 meV on SPINS using pyrolytic graphite (PG) for the monochromator and analyzer. We use the tetragonal notation to index diffraction features throughout this paper. All measurements were done in the (hhl) zone of reciprocal space.

 0031-9007/97/79(13)/2514(4)$10.00

For $La_{2-x}Sr_xNiO_{4+\delta}$ with excess hole concentration $\epsilon = x + 2\delta$, charge order and spin order are characterized by wave vectors $(\epsilon, \epsilon, 1)$ and $(\frac{1}{2} + \frac{1}{2}\epsilon, \frac{1}{2} + \frac{1}{2}\epsilon, 0)$, respectively [5,6]. The spin wave vector $\frac{1}{2}\epsilon$ from the antiferromagnetic reciprocal point $(\frac{1}{2}, \frac{1}{2}, 0)$, being half of ϵ of charge modulation is the signature of charge stripes as magnetic antiphase domain walls [5,6,14]. We consistently found $\epsilon = 0.333(2)$ for $La_{5/3}Sr_{1/3}NiO_4$, as shown in Figs. 1 and 4(a). ϵ was not dependent on temperature (T) [see Fig. 4(a)]. This contrasts with the considerable temperature dependence of ϵ when $\epsilon < \frac{1}{3}$ [6,7] and indicates the stability of the $\epsilon = \frac{1}{3}$ modulation. Figure 1 shows $(\frac{1}{3}, \frac{1}{3}, l)$ scans at various temperatures. Even integer weak l peaks are purely magnetic because they were not detected by electron diffraction [5]. For odd integer l, charge-order scattering is dominant [15]. The superlattice peaks have long tails along l, indicating the quasi-two-dimensionality of structural and spin correlations. Finite repulsive Coulomb interaction will favor a stacking of charge stripe layers in such a way as to minimize the Coulomb interaction. Such a stripe pattern consistent with the superlattice peaks is illustrated at the upper right corner. Notice that all charge stripes in all layers are centered between Ni and O atoms [16].

In Fig. 1, the relative ratios of the peak intensities vary in different T regimes. This led us into detailed measurements of those superlattice peak intensities as a function of T. Figure 2 summarizes the results [in (a), (b), and (c)] along with a bulk susceptibility measurement $d(\chi T)/dT$ [in Fig. 2(d)]. The onset of the superlattice peaks—especially the $(\frac{1}{3}, \frac{1}{3}, 5)$ reflection—at ~240 K, shown in Fig. 2(a), signals the development of the localization of the holes on a time scale $\tau > 2\hbar/\Delta E \sim 5$ ps set by the energy resolution of the instrument. Upon cooling, however, they develop not as an ordinary phase transition, but with an unusually slow rate followed by a fast enhancement at ~200 K. As T decreases further down to 10 K, the peaks continue to grow. At T lower than 40 K, the $(\frac{1}{3}, \frac{1}{3}, 1)$ peak decreases. The existence of the three T regions below 239 K is clearer in the plot of the ratio of the $(\frac{1}{3}, \frac{1}{3}, 1)$ peak intensity to the $(\frac{1}{3}, \frac{1}{3}, 5)$ one as depicted in Fig. 2(b). These three distinct phases are denoted as phases I, II, and III with decreasing T order. Figure 2(c) shows the T dependence of the pure spin contribution to the $(\frac{1}{3}, \frac{1}{3}, 0)$ peak. The contribution of the long tail of the $(\frac{1}{3}, \frac{1}{3}, 1)$ charge peak to the $(\frac{1}{3}, \frac{1}{3}, 0)$ peak was assumed to be the same as that at $(\frac{1}{3}, \frac{1}{3}, 0.3)$ and subtracted. The nonzero intensity below ~190 K demonstrates that the spin ordering occurs in phases II and III, but not in phase I ($190 < T < 239$ K).

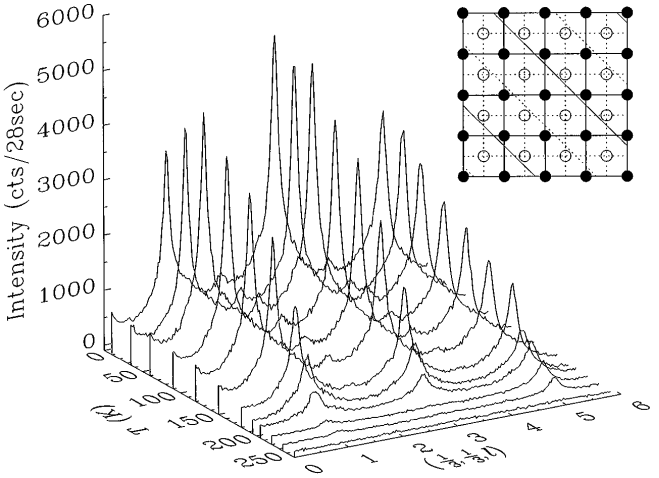

FIG. 1. Neutron diffraction data along $(\frac{1}{3}, \frac{1}{3}, l)$ at a series of temperatures. Data were taken on BT2 with collimations of 60′-40′-40′-80′. Energy resolution was 1.4(1) meV. Typical error was 5% of the intensity. Backgrounds were determined by the measurement at 300 K and were subtracted. At the upper right corner is a stripe pattern for $\epsilon = \frac{1}{3}$ drawn. Filled and open circles indicate Ni sites in one NiO_2 plane and in an adjacent plane, respectively. Square lines, solid and dotted, are the square lattices of Ni atoms. Diagonal lines, solid and dotted, indicate positions of charge stripes in each plane.

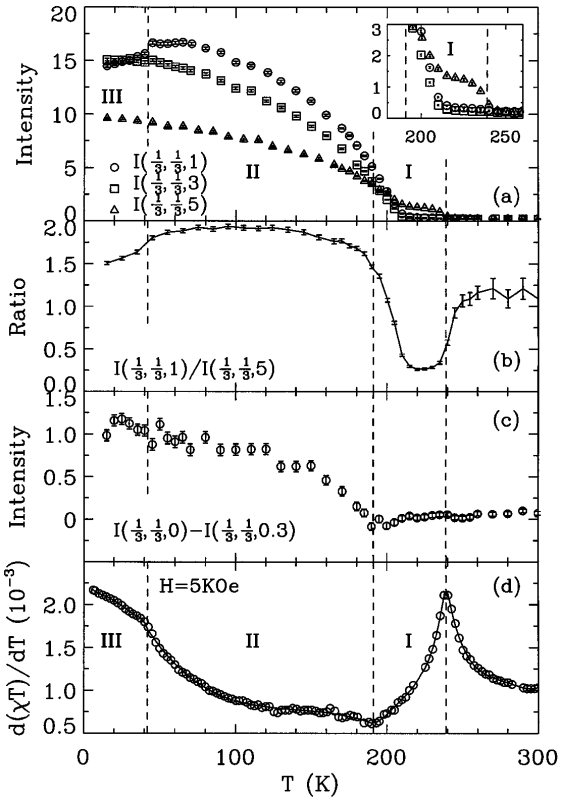

FIG. 2. Elastic neutron scattering intensities of several superlattice peaks and bulk susceptibility data. The energy resolution for the neutron scattering measurements on SPINS was 0.28(2) meV with collimations of open-40′-40′-open. (a) Temperature dependences of the superlattice peak intensities at $Q = (\frac{1}{3}, \frac{1}{3}, 1)$, $(\frac{1}{3}, \frac{1}{3}, 3)$, and $(\frac{1}{3}, \frac{1}{3}, 5)$. The data are in arbitrary units. (b) Ratio of the $(\frac{1}{3}, \frac{1}{3}, 1)$ peak intensity to $(\frac{1}{3}, \frac{1}{3}, 5)$ peak. (c) Temperature dependence of the magnetic superlattice peak intensity. Units are the same as those in (a). (d) $d(\chi T)/dT$ in enu/mole. The line is a guide to the eye.

Anomalies in $d(\chi T)/dT$, shown in Fig. 1(d), establish that the charge-spin correlations in the three phases are static on a time scale more than a few seconds. No thermal hysteresis was observed in any of the measurements, suggesting the phase transitions are continuous.

Interesting aspects of the three phases were discovered in elastic Q scans along the $(hh0)$ and $(00l)$ directions. The $(hh0)$ scan investigates *longitudinal* correlation of translational ordering of stripes along the perpendicular direction to the stripes in the NiO_2 plane. Figure 3(a) shows representative in-plane $(hh1)$ scans, which probe in-plane structural correlations due to charge order. Note that the peak is resolution limited in phases II and III but in phase I it is significantly broader than the q resolution. Thus, the in-plane charge correlation is much shorter in phase I than in phases II and III where the correlation is quasi-long-range. In contrast, the out-of-plane scans shown in Fig. 3(b) are much broader than the q resolution for all phases. Quantitative values of those correlation lengths were obtained by fitting the data at each T to a Lorentzian convoluted with the instrumental resolution function. The fits are drawn as solid lines in Fig. 3, and ϵ, in-plane charge (ξ_a^C) and spin (ξ_a^S) correlation lengths, and out-of-plane charge (ξ_c^C) and spin (ξ_c^S) correlation lengths are plotted in Fig. 4. For all $T < 239$ K, ξ_c^C and ξ_c^S are shorter than $2.5c$, indicating that the quasi-two-dimensionality of both charge and spin correlations remains intact in all three phases. A dramatic difference between the low-T phases (II and III) and the higher-T phase (I) is manifested in the in-plane charge correlation. As illustrated in Fig. 4(b), the in-plane charge correlation is quasi-long-range in phases II and III ($\xi_a^C \sim 350$ Å), which is consistent with the previous electron diffraction result [5]. However, in phase I, ξ_a^C drastically shortens to $\sim$80 Å, which is about 5 times the characteristic wavelength of charge modulation (16.23 Å). There seem to be only subtle differences between phases II and III, both of which exhibit quasi-long-range in-plane charge correlation. The transition is probably a subtle change of structural distortion associated with the hole lattice. ξ_a^C is about 3 times longer than ξ_a^S, indicating that charge ordering is the driving force in this compound and spin ordering is a parasitic effect. Phase I shows short-range charge order in the absence of spin order, which is drastically different from the other two phases. This intermediate glassy state with short-range charge stripe correlation in between solid states (phases II and III) and a liquid state (a disordered high-T state) may be called a "stripe glass."

As in $d(\chi T)/dT$, specific heat (C) exhibits a distinct anomaly at the liquid-glass transition at 239 K and a small kink at the glass-solid transition at 190 K [10], which resembles that seen in a liquid crystal [17]. This indicates that the majority of excess holes localizes into domain walls below 239 K even though the longitudinal correlation of the holes remains short range. As a result, the entropy removed through the glass-solid transition at 190 K is reduced, together with the anomaly. Preliminary inelastic neutron scattering measurements [18] show that low energy charge-spin fluctuations below 3 meV are strongest at $\sim$200 K, at which the correlations become quasi-long-range. Specific heat is sensitive to fluctuations with characteristic energy of order k_BT. Hence, the

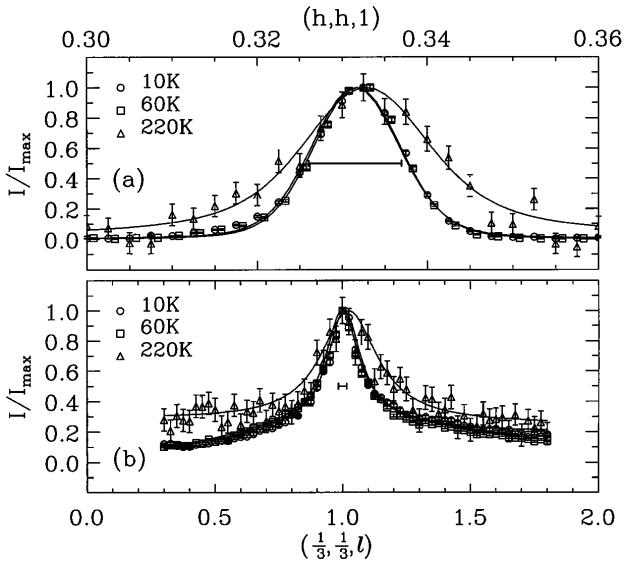

FIG. 3. (a) Representative elastic $(hh1)$ scans for phase I (220 K), phase II (60 K), and phase III (10 K). (b) Representative elastic $(\frac{1}{3}, \frac{1}{3}, l)$ scans in each phase taken from Fig. 3. Solid lines in (a) and (b) are explained in the text. Q resolutions are drawn as bars.

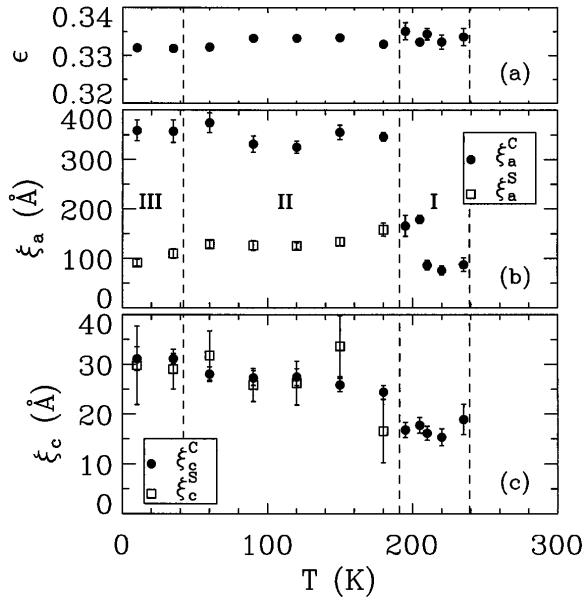

FIG. 4. ϵ and correlation lengths versus temperature. T dependence of (a) ϵ obtained from optimal peak positions of $(\frac{1}{3}, \frac{1}{3}, 1)$ peaks, (b) in-plane correlation lengths, ξ_a^C (charge) and ξ_a^S (spin), obtained by fitting $(\frac{1}{3} + h, \frac{1}{3} + h, 1)$, and $(\frac{1}{3} + h, \frac{1}{3} + h, 0)$ scans, respectively, and (c) out-of-plane correlation lengths, ξ_c^C (charge) and ξ_c^S (spin), obtained by fitting $(\frac{1}{3}, \frac{1}{3}, 1 + l)$ and $(\frac{1}{3}, \frac{1}{3}, 2 + l)$ scans.

distinct specific heat anomaly and the weakness of neutron scattering cross section below 3 meV at 239 K (~20 meV) imply that the characteristic energy of charge fluctuations in the stripe glass state is much higher than 3 meV.

The short-range translational ordering and the specific heat behavior are reminiscent of the 2D glass in 2D melting. Missing in this connection is the orientational order parameter. The 2D glass in 2D melting is characterized by short-range positional order and quasi-long-range orientational order, and has been tested for various real systems such as liquid crystals [19], vortex states of layered cuprate superconductors [20], and doped charge-density-wave compounds [21]. The nematic phase in the liquid crystal has the strongest similarity with the stripe glass in the sense that both of them have twofold symmetry [22]. The orientational order parameter in such systems is an average orientation of stripes and molecules. The difference is, however, that the stripes can have various lengths, whereas molecules in nematic phase have the same length. One might think that the orientational order parameter for the stripes can be measured by *transverse* scans. However, when the stripes are of various lengths even though they are aligned along a common axis, the broadening of transverse scan peaks due to short stripes overshadows the characteristic width due to the orientational order and makes it nearly impossible to extract orientational order parameter from the scans. Nonetheless, the 2D nature of charge order in $La_{5/3}Sr_{1/3}NiO_4$ and the presence of an intermediate state with short-range ordering show the strong similarity of the stripe glass with the 2D glass state. It remains in question as to whether or not such an intermediate glass state in a $La_{2-x}Sr_xNiO_4$ system exists only when $x = \frac{1}{3}$. More experimental studies on $x > \frac{1}{3}$ compounds, especially for $x = \frac{1}{2}$ where bulk measurements show distinct anomalies, as well as theoretical studies, are needed to understand the commensurability effect in the system.

The impurity potential of Sr ions may play an important role in the melting transition of the charge stripes. Sr ions are distributed randomly on the La sites in the La-O layers and can provide pinning potentials for the charge ordering with stripe modulation. These point-defect-like Sr ions can be pinning centers for the translational ordering of the charge stripes, but are naturally inefficient in pinning the orientational ordering of charge stripes. This pinning effect of Sr dopants may be responsible for a stripe glass at intermediate temperatures $190 < T < 239$ K, where the mechanism for producing stripe phase does not dominate the impurity potential and thermal fluctuations. In that phase, most of the holes localize to form strings (possibly maintaining orientational ordering), but the lengths of the strings are short. Upon further cooling, these short strings of holes line up straight to form ordered stripes. Because of the frozen defects, there would be defect regions where two stripes merge into one stripe to form a "double-fork" stripe defect. Such defects would create topological spin frustration, while only producing a small local perturbation of the charge stripe order. This type of stripe defect may be responsible for the shorter correlation of spin than that of charge in phases II and III.

In summary, $La_{2-x}Sr_xNiO_4$ exhibits, at $x = \frac{1}{3}$, unique behaviors which are typical for melting in two dimensions. Among three successive transitions upon cooling, the first two transitions are the continuous transitions of the liquid-glass-solid states of quasi-2D hole ordering. We also presented "consistent" evidences, namely order parameter and correlation length measurements, showing that charge ordering is the driving force in this material.

We have benefited greatly from discussions with P. A. Anderson, C. L. Broholm, C. H. Chen, B. I. Halperin, Y. Ijiri, P. Littlewood, and O. Zachar. Work at SPINS is based upon activities supported by the National Science Foundation under Agreement No. DMR-9423101.

[1] J. Zaanen *et al.*, Phys. Rev. B **40**, 7391 (1989); M. Inui *et al.*, Phys. Rev. B **44**, 4415 (1991).
[2] V. J. Emery *et al.*, Physica (Amsterdam) **209C**, 597 (1993); M. I. Salkola *et al.*, Phys. Rev. Lett. **77**, 155 (1996).
[3] J. M. Tranquada *et al.*, Nature (London) **375**, 561 (1995).
[4] S-W. Cheong *et al.*, Phys. Rev. Lett. **67**, 1791 (1991).
[5] C. H. Chen *et al.*, Phys. Rev. Lett. **71**, 2461 (1993).
[6] J. M. Tranquada *et al.*, Phys. Rev. Lett. **73**, 1003 (1994).
[7] J. M. Tranquada *et al.* (unpublished).
[8] O. Zachar *et al.*, cond-mat/9702055, 1997.
[9] S-W. Cheong *et al.*, Phys. Rev. B **49**, 7088 (1994).
[10] A. P. Ramirez *et al.*, Phys. Rev. Lett. **76**, 447 (1996); R. Burriel *et al.* (unpublished).
[11] E. J. W. Verwey *et al.*, Physica (Amsterdam) **8**, 979 (1941).
[12] Y. Tomioka *et al.*, Phys. Rev. Lett. **74**, 5108 (1995).
[13] J. M. Kosterlitz and D. J. Thouless, J. Phys. C **6**, 118 (1973); B. I. Halperin and D. R. Nelson, Phys. Rev. Lett. **41**, 121 (1978).
[14] S. M. Hayden *et al.*, Phys. Rev. Lett. **68**, 1061 (1992).
[15] The odd l peaks are magnetic as well as structural. However, considering the relative weakness of purely magnetic even l peaks and the different behavior of the odd l peaks in order parameter measurements and in correlation lengths from those of the even l peaks, we conclude that charge-order scattering is dominant in the odd l peaks.
[16] The possibility of an anisotropic distribution of holes around Ni ions is discussed in Ref. [17]. Here we assumed that each plane has the same stripe pattern. If this assumption is weakened, a pattern in which stripes in layers alternate between Ni- and O-centered positions is also possible.
[17] J. Zaanen *et al.*, Phys. Rev. B **50**, 7222 (1994).
[18] S.-H. Lee *et al.* (unpublished).
[19] C. C. Huang *et al.*, Adv. Phys. **42**, 343 (1993).
[20] D. G. Grier *et al.*, Phys. Rev. Lett. **66**, 2270 (1991).
[21] H. Dai *et al.*, Phys. Rev. Lett. **69**, 1576 (1992).
[22] P. G. de Gennes and J. Prost, *The Physics of Liquid Crystals* (Clarendon Press, Oxford, 1993).